Mon. Not. R. Astron. Soc. **000**, 1–?? (2012) Printed 17 October 2012 (MN LaTeX style file v2.2)

arXiv:1210.4162v1 [astro-ph.HE] 15 Oct 2012

Neutrino Acceleration by Bulk Matter Motion and Explosion Mechanism of Gamma-Ray Bursts

Yudai Suwa[1]*
[1] *Yukawa Institute for Theoretical Physics, Kyoto University, Oiwake-cho, Kitashirakawa, Sakyo-ku, Kyoto, 606-8502, Japan*

draft version on 17 October 2012

ABSTRACT
The neutrino annihilation is one of the most promising candidates for the jet production process of gamma-ray bursts. Although neutrino interaction rates depend strongly on the neutrino spectrum, the estimations of annihilation rate have been done with an assumption of the neutrino thermal spectrum based on the presence of the neutrinospheres, in which neutrinos and matter couple strongly. We consider the spectral change of neutrinos caused by the scattering by infalling materials and amplification of the annihilation rate. We solve the kinetic equation of neutrinos in spherically symmetric background flow and find that neutrinos are successfully accelerated and partly form nonthermal spectrum. We find that the accelerated neutrinos can significantly enhance the annihilation rate by a factor of ~ 10, depending on the injection optical depth.

Key words: acceleration of particles – accretion, accretion discs – gamma-ray burst: general – neutrinos – radiative transfer

1 INTRODUCTION

The neutrinos play a very important role in the extremal condition in astrophysics. Although photons are strongly coupled with the matter in the dense material, neutrinos are able to escape due to its weak coupling with the matter. Therefore, neutrinos can be an important cooling source and significantly affect the dynamics. In addition, they can even be a heating source in several cases, e.g., the neutrino capture process in the core-collapse supernovae (CCSNe) (Bethe 1990) and the neutrino annihilation in the central engine of gamma-ray bursts (GRBs) (MacFadyen & Woosley 1999). In the hot (temperature $T \gtrsim 1$MeV) and dense (density $\rho \gtrsim 10^{11}$ g cm^{-3}) gas, even neutrinos are trapped and thermalized so that the temperature of neutrinos becomes coincident with that of the matter. The surface where the neutrinos are decoupled from the matter is called "neutrinosphere", which is analogous to a photosphere of photons.

Due to the existence of neutrinosphere, the spectrum of neutrinos is often assumed to be a thermal (Fermi-Dirac) distribution. However, we know, by the numerous studies of photons, that the radiation spectrum can easily be deformed from the thermal one in the propagation regime. The nonthermal radiation spectrum can be produced by the nonthermal spectrum or the different temperature of the scattering bodies. As for the case of photons, the processes that produce the nonthermal spectrum by electron scattering are called thermal Compton (see, e.g., Rybicki & Lightman 1979) and bulk Compton processes (Blandford & Payne 1981). The former process is driven by the electrons with different temperature from photons, while the latter is induced by electrons with the inhomogeneous velocity field. In the case of neutrinos, the bulk motion of scattering materials could lead to the similar effect and produce nonthermal component of neutrinos, which was not investigated so far.[1]

Neutrino interactions with matter strongly depend on the energy of neutrinos, i.e., the cross section $\sigma \propto \varepsilon_\nu^2$ with ε_ν being the neutrino energy. Thus, little difference of spectrum (especially at the high-energy region) could lead significantly different dynamics. The neutrino capture and the neutrino annihilation are critically important for the shock revival of CCSNe and the jet production of GRBs,[2] respectively. As for CCSNe, there are significant efforts for solving Boltzmann equation of neutrinos with hydrodynamics

---

* E-mail: suwa@yukawa.kyoto-u.ac.jp

[1] Indeed, the term which is related to this effect is included in the numerical simulations that solve the neutrino Boltzmann equation. However, due to the small radial velocity in the postshock region, this effect plays significantly minor role in the context of the core-collapse supernovae. Thus, there was no study focusing on this effect. On the other hand, we consider the free-fall background flow without the shock in this paper so that the radial velocity is large enough to make nonthermal component.

[2] Note that there are other alternatives for jet production mechanism of GRBs. Among them, another promising candidate is the Poynting dominated jet, which is driven by the magnetic field.

numerically because the explosion mechanism (particularly delayed-explosion scenario) tremendously relies on neutrino physics. Since the neutrinospheres for CCSNe are basically spherical (deformation is moderate if the rotation is not very rapid), the neutrino transfer can be solved with spherical symmetric background, which is reachable even for the current computer resources. In fact, hydrodynamic simulations together with neutrino Boltzmann equation have been done in spherical symmetric case (e.g., Liebendörfer et al. 2001; Sumiyoshi et al. 2005).[3] On the other hand, the central engine of GRBs is essentially asymmetric (e.g., the compact object and the accretion disk system) so that neutrino transfer should be solved with multi-dimensional treatment. Although there are a few attempts to solve the neutrino radiative transfer in multidimensional manner (e.g., Dessart et al. 2009; Sumiyoshi & Yamada 2012), the long-term dynamical simulation is still too computationally expensive so that the numerical solutions of full Boltzmann equation are not accessible at the moment. Because of these facts, the neutrino interactions in the central engine of GRBs are introduced with plenty of assumptions. One of them is the thermal spectrum.

Among the accretion disk models, the neutrino-dominated accretion flow (NDAF), in which copious neutrinos are emitted and dominates the cooling, is often discussed as a candidate of the central engine of GRBs. Popham et al. (1999) derived the disk structure and neutrino luminosity by solving the group of equations of state, hydrodynamics, thermodynamics and microphysics in detail. The energy conversion efficiencies become extremely high (the annihilation luminosity $L_{\nu\bar{\nu}}$ becomes as large as $\sim 10^{53}$ erg s^{-1}) for the mass accretion rate $\dot{M} = 10 M_\odot$ s^{-1}. However, their results are too optimistic, as they ignored neutrino opacity and overestimated the neutrino luminosity. Di Matteo et al. (2002) showed that the effect of neutrino opacity becomes significant for $\dot{M} > 1 M_\odot$ s^{-1}, and recalculated the annihilation rate including the concept of neutrinosphere. They demonstrated that the $L_{\nu\bar{\nu}}$ increases up to its maximum value of $\sim 10^{50}$ erg s^{-1} at $\dot{M} \approx 1 M_\odot$ s^{-1} and decrease for larger $\dot{M}$. Thus they concluded that the neutrino annihilation in NDAF is not a sufficient mechanism for liberating large amount of energy. Nagataki et al. (2007) performed axisymmetric simulation of the collapsar and found that the neutrino annihilation is less important than neutrino capture as a heating source. These negative results could come from the assumption employed in their calculation, i.e., they neglected the neutrino emission from the region with neutrino optical depth $\tau \gtrsim 1$ and employed a thermal distribution with a single temperature for the neutrino spectrum.[4]

In this paper, multiple scattering of neutrinos and the acceleration (i.e., up scattering) in a fluid flow is considered. We investigate the impact to the pair-annihilation rate by accelerated component of neutrinos. Note that although in this paper we consider the parameter regime for the collapsar scenario that is one of promising candidates of long-duration GRBs, the neutrino acceleration process, however, is viable for the central engine of short GRBs. Thus, the following is applicable both for long and short GRBs. The rest of this paper is organized as follows. In §2, we briefly review the concept of neutrinosphere. In §3, we describe the radiative transfer equation for neutrinos and show that its solution contains nonthermal component. In §4 we investigate the effect of nonthermal component of neutrino on the neutrino-annihilation rate. We summarize our results and discuss their implications in §5.

2 NEUTRINOSPHERES

There are three types of neutrinosphere, which are determined by the different micro processes (see Raffelt 2001). Here, we explain these "neutrinospheres" one by one:

- **Number sphere**: The optical depth by the emission and absorption of neutrinos is about unity. As for $\nu_{\rm e}$ and $\bar{\nu}_{\rm e}$, the electron/positron capture and its inverse process (i.e., $\nu_{\rm e}$+n $\leftrightarrow$ p+e$^-$ and $\bar{\nu}_{\rm e}$+p $\leftrightarrow$ n+e$^+$) are important processes. As for ν_X, which represents heavier leptonic neutrinos and their antineutrinos (i.e., $\nu_\mu, \nu_\tau, \bar{\nu}_\mu$, and $\bar{\nu}_\tau$), the pair production/annihilation processes (i.e., $\nu\bar{\nu} \leftrightarrow \gamma\gamma$, $\nu\bar{\nu} \leftrightarrow e^+e^-$, $NN \leftrightarrow NN\nu\bar{\nu}$) determine the opacity.
- **Energy sphere**: The inelastic scattering by electron is important process here. The electrons receive the energy from neutrinos because the electron rest mass energy (511 keV) is much smaller than the typical neutrino energy (~ 10 MeV), which is determined by the matter temperature at the number sphere. Inside the energy sphere the neutrinos are thermalized due to energy transfer with electrons, which are tightly coupled with baryons.
- **Transport sphere**: Beyond the energy sphere, the elastic scattering by nucleons and nuclei is dominant source of the opacity. Because the rest mass energy of these particles is much larger than neutrino energy, these scattering can be treated as the elastic scattering.[5]

As for $\nu_{\rm e}$ and $\bar{\nu}_{\rm e}$, all neutrinospheres provided above are almost coincident so that the spectrum is almost thermal. On the other hand, ν_X has distinct radii of neutrinospheres (Raffelt 2001). Therefore, ν_X could have nonthermal component, which would be produced between energy and transport spheres.

---

[3] Recently, multi-dimensional hydrodynamic simulations with neutrino transfer have been performed by several groups (Buras et al. 2006; Burrows et al. 2006; Bruenn et al. 2009; Suwa et al. 2010) by employing several assumptions to reduce the computational costs. More recently, the development of a full seven-dimensional Boltzmann solver is reported (Sumiyoshi & Yamada 2012).

[4] There are a large number of attempts to amplify the neutrino-annihilation rate. Especially, the effects of (general) relativity are paid attention, such as beaming by relativistic motion and bending by black-hole space time (e.g., Asano & Fukuyama 2000, 2001). The relativistic effects for the structure of NDAF is also discussed recently (Chen & Beloborodov 2007; Zalamea & Beloborodov 2011).

[5] Note that Raffelt (2001) investigated how the recoil term affects the spectrum of ν_X.

3 THE RADIATIVE TRANSFER EQUATION AND ITS SOLUTION

Here we consider the neutrino radiative transfer on the background of hyperaccreting matter. We focus on the region between the energy sphere and the transport sphere, where the scattering by nucleons dominates the opacity.

3.1 Accretion Flow

Here, we briefly describe profiles of matter as a background of neutrino radiative transfer. In this calculation, we employ the spherically symmetric accretion flow in order to mimic the collapsar.

Let $\dot{M}$ be the rate at which matter is accreting, and let its radial inward speed be

$$u(r) = c\left(\frac{r_s}{r}\right)^{1/2}, \tag{1}$$

where c is the speed of light and r_s is the Schwarzschild radius. This free-fall velocity profile makes the implicit assumption that the radiation force on the accreting matter is insignificant or equivalently, that the escaping luminosity is much less than the Eddington value. The scattering optical depth of the flow from a radius r to infinity is given by

$$\tau_{\rm sc} = \int_r^\infty dr' n(r')\sigma(\varepsilon_\nu) = \dot{m}\left(\frac{r_s}{r}\right)^{1/2}, \tag{2}$$

where $n(r)$ is the nucleon number density ($n(r) = \dot{M}/[4\pi r^2 m_p u(r)]$), $\sigma(\varepsilon_\nu)$ is the scattering cross section for neutrino energy ε_ν, and the dimensionless mass accretion rate $\dot{m} = \dot{M}/\dot{M}_{{\rm Edd},\nu}$, respectively. Here, $\dot{M}_{{\rm Edd},\nu}$ is the Eddington accretion rate defined by

$$\dot{M}_{{\rm Edd},\nu} \equiv \frac{L_{{\rm Edd},\nu}}{c^2} = \frac{4\pi G M m_p}{\sigma(\varepsilon_\nu)c}, \tag{3}$$

where $L_{{\rm Edd},\nu}$ is the Eddington luminosity of neutrinos, M is the mass of the central object, m_p is the proton mass, and G is the gravitational constant. Since $\dot{m}$ depends on the neutrino energy, we introduce $\dot{m}_{kT}$, which represents $\dot{m}$ for $\varepsilon_\nu = kT$ with k and T being Boltzmann constant and the matter temperature.

For supercritical accretion into black holes ($\dot{m} \geqslant 1$), it is evident from Eq. (2) that there should be regions in the flow where the neutrinos propagate diffusively. For our problem, it is convenient to use not $\tau_{\rm sc}$ but the effective optical depth

$$\tau \equiv \frac{3}{2}\frac{u(r)}{c}\tau_{\rm sc}(r) = \frac{3}{2}\dot{m}\frac{r_s}{r} = \frac{3}{2}\dot{m}_{kT}\left(\frac{\varepsilon_\nu}{kT}\right)^2\frac{r_s}{r}. \tag{4}$$

This value will replace the radial coordinate r in the radiative transfer equation in §3.2. It should be noted that τ depends on ε_ν as well due to the energy dependence of the scattering cross section. In addition, we introduce the dimensionless neutrino energy as

$$x \equiv \frac{\varepsilon_\nu}{kT}. \tag{5}$$

3.2 Radiative Transfer Equation

Now we proceed to write down and solve the radiative transfer equation. For the kinetic equation, we start from equation (18) of Blandford & Payne (1981) for the neutrino occupation number $f_\nu(\mathbf{r}, \varepsilon_\nu)$,

$$\begin{aligned}\frac{\partial f_\nu}{\partial t} + \mathbf{u}\cdot\nabla f_\nu = \; & \nabla\cdot\left(\frac{c}{3\kappa(\varepsilon_\nu)}\nabla f_\nu\right) \\ & + \frac{1}{3}(\nabla\cdot\mathbf{u})\varepsilon_\nu\frac{\partial f_\nu}{\partial \varepsilon_\nu} + j(\mathbf{r}, \varepsilon_\nu),\end{aligned} \tag{6}$$

where $\kappa(\mathbf{r}) \equiv n(\mathbf{r})\sigma(\varepsilon_\nu)$ is the inverse of the scattering mean free path and $j(\mathbf{r}, \varepsilon_\nu)$ is the emissivity. Here, we neglect the recoil term, which affects the neutrino spectrum only for the regime of $\varepsilon_\nu \gtrsim m_p c^2 \sim 1$ GeV (typical neutrino energy is ~ 10 MeV). Substituting the inflow velocity $\mathbf{u} = -u(r)\hat{\mathbf{r}}$, where $\hat{\mathbf{r}}$ is the radial unit vector, and taking into account the spherical symmetry, Eq. (6) becomes

$$\frac{\partial f_\nu}{\partial \tilde{t}} = \tau\frac{\partial^2 f_\nu}{\partial \tau^2} - \left(2\tau + \frac{3}{2}\right)\frac{\partial f_\nu}{\partial \tau} - \frac{1}{2}x\frac{\partial f_\nu}{\partial x} + \frac{\tau j}{3c\kappa(x)}, \tag{7}$$

where $\tilde{t} \equiv 3c\kappa t/\tau$ is the dimensionless time. The dimensionless spectral energy flux $F(r, \varepsilon_\nu)$ (Blandford & Payne 1981) is written in the new variables as

$$F(\tau, x) \propto x^2\left(\frac{2\tau}{3\dot{m}_{kT}}\right)^{1/2}\left[\left(\frac{2\tau}{3} + 1\right)\frac{\partial f_\nu}{\partial \tau} + \frac{1}{3}x\frac{\partial f_\nu}{\partial x}\right]. \tag{8}$$

Note that we are interested in the spectrum at a certain radius, not the optical depth, which depends on both the radius and neutrino energy. Thus, by combining Eqs. (4) and (8), we evaluate the spectral energy flux at a certain radius as

$$F(\tau, x)|_r \propto x^3\left[\left(\frac{2\tau}{3} + 1\right)\left.\frac{\partial f_\nu}{\partial \tau}\right|_r + \frac{1}{3}x\frac{\partial f_\nu}{\partial x}\right]. \tag{9}$$

3.3 Analytic Solution

In this subsection, we neglect the last term in the right hand side of Eq. (7) in order to obtain an analytic solution. This is because this term changes the number of neutrinos, which would have minor contribution between the energy sphere and transport sphere (see §2). Following Payne & Blandford (1981), we solve Eq. (7) using variable separation with the form

$$f_\nu(\tau, x) = R(\tau)\tau^{5/2}x^{-\alpha}. \tag{10}$$

Here α becomes an eigenvalue of the following confluent hypergeometric differential equation

$$\tau\frac{{\rm d}^2 R}{{\rm d}\tau^2} + \left(\frac{7}{2} - 2\tau\right)\frac{{\rm d}R}{{\rm d}\tau} + \left(\frac{\alpha - 10}{2}\right)R = 0. \tag{11}$$

The physical solution of Eq. (11) fulfills a constant spectral flux of neutrinos as $\tau \to 0$ and adiabatic compression of the neutrinos $\tau \to \infty$. The relevant solution can be evaluated as an infinite sum of generalized Laguerre polynomials $L_n^{5/2}(2\tau)$. The corresponding eigenvalues α_n are given by

$$\alpha_n = 4n + 10; \qquad n = 0, 1, 2, ... \tag{12}$$

These values are different from Payne & Blandford (1981) because the cross section depends on energy for the current case. Note that this spectral index does not imply the observable spectrum at a certain radius because τ depends on not only a radius but also the considered neutrino energy (see Eq. 4). In order to obtain a spectral flux at r, we should multiply Eq. (9) by x^3 because $\partial f_\nu/\partial\tau|_r \propto \tau^{3/2} \propto x^3 r^{-3/2}$

for $\tau \to 0$ (the other terms drop faster than this term). Thus, the hardest spectral component (i.e., $n = 0$) of F becomes $\propto \varepsilon_\nu^{-4}$.

In principle, the global solution of Eq. (7) can be given by summing up infinite series expressed by $L_n^{5/2}(2\tau)x^{-\alpha_n}$ with coefficients determined by the boundary condition. In fact, Payne & Blandford (1981) gave the analytic solution with the delta-function distribution function at the injection optical depth, in which all coefficients are expressed by generalized Laguerre Polynomials and Gamma functions (see Eqs. 10 and 11 in their paper). However, the analytic expression for the arbitrary boundary condition is not always representable using known functions. Thus, in the following we solve Eq. (7) numerically with the thermal distributions of neutrinos at the energy sphere as a boundary condition.

3.4 Numerical Solution

In this subsection, we present our numerical solution of Eq. (7). The last term is omitted again because the interested region is between the energy sphere and transport sphere (see §2). We use the relaxation method for the boundary problem (e.g., Press et al. 1992), in which the stationary solution is achieved by infinitely long exposure of the time dependent equation.

In solving Eq. (7), we change this equation to a finite-difference form using

$$\frac{\partial^2 f_\nu}{\partial \tau^2} = \frac{2}{\delta\tau_i + \delta\tau_{i+1}}\left(\frac{f_\nu^{i+1,j} - f_\nu^{i,j}}{\delta\tau_{i+1}} - \frac{f_\nu^{i,j} - f_\nu^{i-1,j}}{\delta\tau_i}\right) \quad (13)$$

$$\frac{\partial f_\nu}{\partial \tau} = \frac{f_\nu^{i+1,j} - f_\nu^{i-1,j}}{\delta\tau_i + \delta\tau_{i+1}}, \quad (14)$$

$$\frac{1}{2}x\frac{\partial f_\nu}{\partial x} = \frac{1}{2}x_j\frac{f_\nu^{i,j+1} - f_\nu^{i,j-1}}{\delta x_j + \delta x_{j+1}}, \quad (15)$$

where i and j denote the grid point of τ and x, respectively. The grid points are determined by the rule as

$$\tau_i = \tau_{i-1} + \delta\tau_i, \quad (16)$$

$$x_j = x_{j-1} + \delta x_j, \quad (17)$$

$$\delta\tau_i = r_\tau \delta\tau_{i-1}, \quad (18)$$

$$\delta x_j = r_x \delta x_{j-1}, \quad (19)$$

where r_τ and r_x are constants larger than unity. We set $\delta\tau_1/\tau_1 = \delta x_1/x_1 = 0.02$. The calculations are performed on a grid of 200 zones for τ from 0.01 up to τ_0 and 500 zones for x from 0.1 to 100. A test calculation and comparison with an exact solution are given in Appendix.

The boundary condition is given at τ_0 as

$$f_\nu(\tau_0, x) = \frac{\tau_0^{5/2}}{x^5}\frac{1}{1+e^x}, \quad (20)$$

where the factor $\tau_0^{5/2}/x^5$ means the correction, which leads to the thermal distribution function at a radius r. In this study, we set the above boundary condition with only one parameter τ_0 for simplicity. In order to make more realistic boundary condition, we should consider the microphysical processes that change the neutrino number and energy in detail, which is beyond the scope of this paper. Here we do not care about the normalization factor because all equations solved in this study are linear to f_ν as we omit the source term j. Needless to say, we should care about the normalization with detailed source term because neutrino is fermion so that there is a significant effect by Pauli blocking for $f \sim 1$.

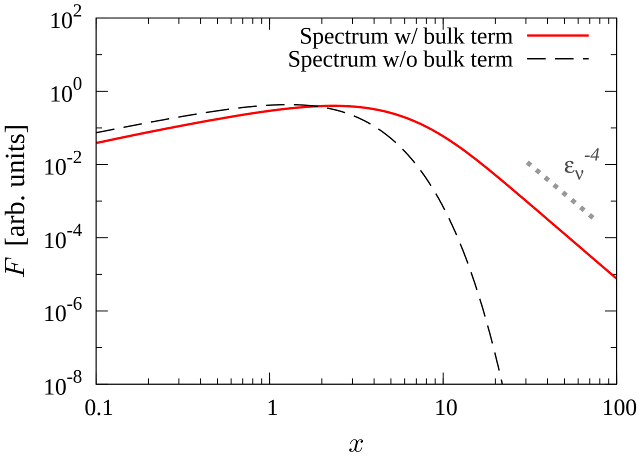

Figure 1. The emergent spectral energy flux estimated by the numerical solution. The boundary condition is given at $\tau_0 = 5$. The correction for the conversion from τ-space to r-space is included (see text for details). The red solid line is the solution of the full equation of Eq. (7), while the black dashed line is the solution of the kinetic equation without the bulk term (i.e., thermal spectrum). The grey dotted line represents the power-law spectrum of ε_ν^{-4}, which is the analytic solution (see text for details).

In Figure 1, we show the numerical solution of the dimensionless spectral energy flux obtained by solving Eqs. (7) and (9). The red solid line represents the emergent spectrum of full equation and the black thin dashed line is spectrum obtained by the kinetic equation *without* bulk term (i.e., $\frac{1}{3}(\nabla\cdot\mathbf{u})\varepsilon_\nu\frac{\partial f_\nu}{\partial \varepsilon_\nu}$ in Eq. 6), that is, a thermal spectrum. One can see that neutrinos are upscattered by the infalling material and the nonthermal spectrum is generated. As indicated by grey-dotted line, the emergent spectrum is power law with ε_ν^{-4} for $x = \varepsilon_\nu/kT \gtrsim 10$, which is consistent with the analytic solution with $n = 0$ obtained in the previous section. In this calculation, the boundary condition is given at $\tau_0 = 5$, where f_ν has a thermal distribution with a temperature, T.[6] The flux is estimated at $\tau = 0.01$, where the spectral evolution is almost completed. The normalization of both spectra is determined by the total number flux, $\int(F/x)dx$, being unity.

We show the different solutions with different τ_0 in Figure 2. It is obvious that higher τ_0 leads to harder spectrum. It should be noted that the position of the energy sphere depends on the elementary process such as $\nu e \leftrightarrow \nu e$, $e^+e^- \leftrightarrow \nu\bar{\nu}$, and NN bremsstrahlung. The first process is related to the thermalization and the others are related to

---

[6] According to numerical simulations of core-collapse supernovae, which include detailed microphysics and the radiative transfer, the temperature of ν_X ranges from 4 MeV to 10 MeV (see Horiuchi et al. 2009, for a collective reference of recent numerical simulations). These values can be used in the case of long GRBs. As for short GRBs, Setiawan et al. (2006) showed that the average energy of ν_X range from $\sim$ 5 MeV to $\sim$ 27 MeV, corresponding to the temperature from $\sim$ 2 MeV to $\sim$ 9 MeV with vanishing chemical potential, similar to values of CCSNe.

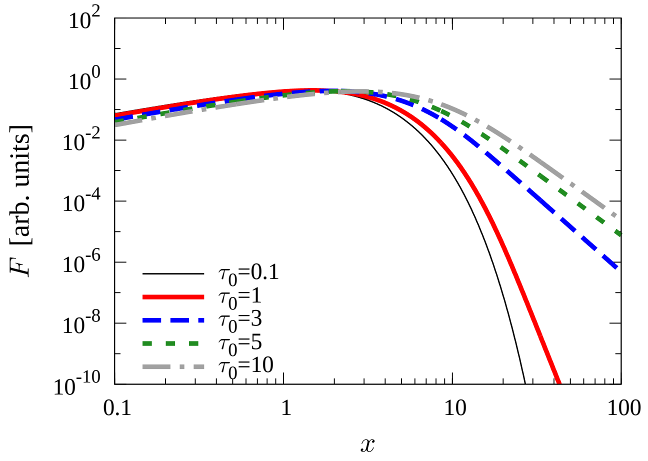

Figure 2. The emergent spectral energy flux with different τ_0 indicated by different lines. The higher τ_0 leads to the harder spectrum due to efficient up-scattering by the infalling material.

both the thermalization and emission/absorption. The dominant thermalization process depends on the background fluid temperature, density, and abundance, which are much beyond the scope of this paper. Thus, we simply parametrize the injection τ_0 and see the dependences on it (see also Raffelt 2001).

4 NON-THERMAL NEUTRINOS AND THEIR ANNIHILATION

Now we move on to estimate the neutrino annihilation rate, which strongly depends on neutrino energy. The energy deposition rate via neutrino-annihilation ($\nu + \bar{\nu} \rightarrow e^+ + e^-$) is given by (Goodman et al. 1987; Setiawan et al. 2006)

$$\dot{E}_{\nu\bar{\nu}} = \mathcal{C} F_{3,\nu} F_{3,\bar{\nu}} \left(\frac{\langle \varepsilon_\nu^2 \rangle \langle \varepsilon_{\bar{\nu}} \rangle + \langle \varepsilon_{\bar{\nu}}^2 \rangle \langle \varepsilon_\nu \rangle}{\langle \varepsilon_\nu \rangle \langle \varepsilon_{\bar{\nu}} \rangle} \right), \tag{21}$$

where $F_{i,\nu} = \int f_\nu \varepsilon_\nu^i \mathrm{d}\varepsilon_\nu$, $\langle \varepsilon_\nu \rangle = F_{3,\nu}/F_{2,\nu}$, and $\langle \varepsilon_\nu^2 \rangle = F_{4,\nu}/F_{2,\nu}$, respectively. The factor $\mathcal{C}$ includes the weak interaction coefficients and the information of the angular distribution of the neutrinos so that to calculate this factor we should determine the geometry of the neutrino-emitting source. Since this factor is expected not to change significantly by including the neutrino acceleration process, we concentrate on the effect of the spectral change from here. For simplicity, we assume the spectrum of ν and $\bar{\nu}$ are identical. Then, we get

$$\dot{E}_{\nu\bar{\nu}} \propto \frac{F_{3,\nu}^2 \langle \varepsilon_\nu^2 \rangle}{\langle \varepsilon_\nu \rangle}. \tag{22}$$

We can evaluate the amplification of the neutrino annihilation rate by the accelerated component of neutrino produced by the bulk motion of background matter using $F_{3,\nu}$, $\langle \varepsilon_\nu \rangle$, and $\langle \varepsilon_\nu^2 \rangle$. By assuming that the neutrino number flux ($F_{2,\nu}$) does not change by including this effect, we get $F_{3,\nu} \propto \langle \varepsilon_\nu \rangle$, then $\dot{E}_{\nu\bar{\nu}} \propto \langle \varepsilon_\nu \rangle \langle \varepsilon_\nu^2 \rangle$ Therefore, we can evaluate the amplification only by $\langle \varepsilon_\nu \rangle$ and $\langle \varepsilon_\nu^2 \rangle$.

Table 1 shows the integrated values of emergent spectrum. It is obvious that both the mean energy $\langle \varepsilon_\nu \rangle$ and the mean-square energy $\langle \varepsilon_\nu^2 \rangle$ increase compared to the thermals spectrum due to up-scattering by the infalling materials. As a result, the neutrino annihilation rate is significantly amplified by the accelerated component. In addition, we show the convergence check with higher resolution in this table (see last two lines). Due to much more expensive numerical cost, we just calculate the model with $\tau_0 = 1$ and confirm the validity of the lower resolution calculation.

Table 1. Properties of numerical solutions

τ_0	N_τ[†]	N_x[‡]	$\frac{\langle \varepsilon_\nu \rangle}{\langle \varepsilon_\nu \rangle_{thermal}}$[§]	$\frac{\langle \varepsilon_\nu^2 \rangle}{\langle \varepsilon_\nu^2 \rangle_{thermal}}$	$\frac{\mathcal{A}}{\mathcal{A}_{thermal}}$[¶]
0.1	200	500	1.01	1.02	1.03
0.2	200	500	1.03	1.05	1.08
0.5	200	500	1.07	1.16	1.24
1.0	200	500	1.16	1.37	1.59
1.5	200	500	1.26	1.65	2.08
2.0	200	500	1.37	1.99	2.73
3.0	200	500	1.60	2.83	4.52
5.0	200	500	1.95	4.49	8.77
7.0	200	500	2.18	5.72	12.5
10.0	200	500	2.43	7.12	17.3
1.0	500	1000	1.16	1.36	1.57
1.0	750	1500	1.16	1.37	1.59

[†] Numerical grids for τ.
[‡] Numerical grids for x.
[§] The average energy of emerged spectrum.
[¶] The amplification of the neutrino-annihilation rate (Eq. 22) compared to the thermal distribution.

5 SUMMARY AND DISCUSSION

In this paper, we consider the spectral change of neutrinos induced by the scattering of the infalling materials and amplification of the annihilation rate, which is one of the well-discussed jet production mechanism of GRBs. We solve the kinetic equation of neutrinos in spherically symmetric background flow and find that neutrinos are successfully accelerated and partly form nonthermal spectrum. We find that the accelerated neutrinos can significantly enhance the annihilation rate by a factor of ~ 10, depending on the injection optical depth.

In this study, we tried to demonstrate the effect of the up-scattering by the bulk motion of the material and just assumed the injection optical depth with parametric manner. More realistic injection is obtained by the insight of the energy sphere, whose position is determined by the neutrino-electron inelastic scattering as follows. The scattering opacity at energy sphere, where the inelastic scattering with electrons freeze out, can be calculated by the ratio of cross section[7],

$$\frac{\tau_{\rm sc}(r_{\rm es})}{\tau_{\rm es}} \sim \frac{n_{\rm N}\sigma_{\rm n}}{n_{\rm e}\sigma_{\rm e}} \sim \frac{2\varepsilon_\nu}{3Y_{\rm e}kT(r_{\rm es})} \tag{23}$$

where $\tau_{\rm es}$ is the optical depth of electron inelastic scattering, $r_{\rm es}$ is the radius of energy sphere, $n_{\rm N}$ and $n_{\rm e}$ are the number density of nucleons (neutrons and protons) and electrons, and $Y_{\rm e} = n_{\rm e}/n_{\rm N}$ is the electron fraction, respectively. Since $\tau_{\rm es}$ is definitely 2/3 at the energy sphere,

$$\tau_{\rm sc}(r_{\rm es}) \sim \frac{4\varepsilon_\nu}{9Y_{\rm e}kT(r_{\rm es})}. \tag{24}$$

The typical temperature of neutrinospheres is $\sim$ 4 MeV (Janka 2001) so that $\tau_{\rm sc}$ is larger than 2/3 for neutrinos of the energy $\varepsilon_\nu \gtrsim 0.6(Y_{\rm e}/0.1)$ MeV. The typical value of $Y_{\rm e}$ is ~ 0.1 at the region where the electron capture is significant so that almost all the neutrinos are trapped by the nucleon elastic scattering at the energy sphere. Although the injection optical depth in this study should be energy dependent as shown above, we neglect this effect for simplicity.

Next, we discuss about the neutrino species. In this paper, we consider the region between the energy sphere and the transport sphere, i.e. the optical depth is larger than unity for the neutrino-nucleon elastic scattering. Note that usually these neutrino spheres are coincident for $\nu_{\rm e}$ and $\bar{\nu}_{\rm e}$ due to the presence of the charged current for these neutrinos so that the neutrino acceleration studied in this paper is possible only for ν_μ, ν_τ and their anti particles. However, for the case of neutron number density being much larger than protons' one, the charged current reaction of $\bar{\nu}_{\rm e}$ ($\bar{\nu}_e + p \to n + e^+$) is negligible so that the reactions relevant to $\bar{\nu}_e$ become similar to those of heavier leptonic neutrinos. The transport opacity for the neutral current scattering processes are given by (Janka 2001)

$$\kappa_{\rm sc} \sim \frac{5\alpha^2+1}{24}\frac{\sigma_0\langle\epsilon_\nu^2\rangle}{(m_{\rm e}c^2)^2}\frac{\rho}{m_{\rm u}}(Y_{\rm n}+Y_{\rm p}). \tag{25}$$

Here $m_{\rm u} \sim 1.66\times10^{-24}$ g is the atomic mass unit, $\alpha = -1.26$, and $Y_{\rm n} = n_{\rm n}/n_N$ and $Y_{\rm p} = n_{\rm p}/n_N$ are the number fractions of free neutrons and protons, i.e., their particle densities normalized to the number density of nucleons, respectively. In cases of $\nu_{\rm e}$ and $\bar{\nu}_{\rm e}$ also the charged-current absorption on neutrons and protons, respectively, need to be taken into account due to their large cross sections. The absorption opacity is (Janka 2001)

$$\kappa_a \sim \frac{3\alpha^2+1}{4}\frac{\sigma_0\langle\epsilon_\nu^2\rangle}{(m_{\rm e}c^2)^2}\frac{\rho}{m_{\rm u}}\left\{\begin{array}{c}Y_{\rm n}\\ Y_{\rm p}\end{array}\right\}. \tag{26}$$

From Eqs. (25) and (26) the scattering dominates the opacity for $\bar{\nu}_{\rm e}$ provided $Y_{\rm p} < 0.26$. In this case, the transport sphere and number sphere (Janka 1995; Raffelt 2001) separate from each other for $\bar{\nu}_{\rm e}$. The time stationary solutions of hyperaccreting flow imply that Y_e can be as small as ~ 0.1 (Kawanaka & Mineshige 2007), similar to the case of core-collapse supernova (just above the neutrino sphere, $Y_e \sim 0.05 - 0.1$). Therefore, it is expected that the acceleration of $\bar{\nu}_{\rm e}$ would naturally occur in the collapsar system.

Our finding suggests that the detectability of MeV neutrinos is also enhanced because the expected detection number $\propto F_{2,\nu}\langle\varepsilon_\nu^2\rangle$. If this neutrino acceleration works only for ν_X, the neutrino oscillation would produce $\bar{\nu}_{\rm e}$, which is main observable for walter Čerenkov detectors. Suwa & Murase (2009) estimated the expected number from the hyperaccreting accretion flow with thermal spectrum of $kT = 3$ MeV and argued that GRBs are observable for $\lesssim$ a few Mpc by Super-Kamiokande and several Mpc by Mton detector. The neutrino acceleration process thought in this paper would push out the detectable horizon of MeV neutrino farther.

At last, we comment on our assumptions in this study. Firstly, we employed the diffusion limit for whole region, which is not valid for optically thin region, $\tau_{\rm sc} \lesssim 1$. The conclusion, however, does not change if we somehow include effects of optically thinness, since the spectral evolution is determined by the region $\tau_{\rm sc} \gtrsim 1$. Secondly, we dropped out the recoil term from the kinetic equation. The average energy of neutrinos is not affected by this because the recoil term changes the spectrum for $\gtrsim 1$ GeV which is much higher than the typical energy of neutrino spectrum. Thus, if we include the recoil term (that is much more complicated than terms included in this study), the conclusion does not change very much. Thirdly, we fixed the background matter flow as free fall. The energy gain of neutrinos must come from the matter so that the back reaction should be included when the total energy of neutrinos reaches as large as the matter kinetic energy. To compare these two quantities, more detailed source term is necessary. The final answer can be obtained by solving neutrino radiation hydrodynamic equations in self-consistent way, which is far beyond the scope of this simple study. Fourthly, we omitted the relativistic effects, e.g., the Doppler shift and gravitational redshift. In order to include these effects, we should reformulate by covariant formulation of the radiative transfer in self-consistent way. One can find such a formulation in Shibata et al. (2011). Finally, the spherical symmetry is also one of the largest assumption in this study. This assumption is partially valid because NDAF solution has large disk height due to the large contribution of gas for pressure (otherwise if the disk is supported by the centrifugal force, the disk height is almost negligible compared to the disk radius). Considering the disk structure, neutrinos can escape from the accretion flow to the vertical direction before the spectral evolution completes. Whether this effect amplifies or suppresses the neutrino annihilation is not trivial because there are two possible opposite effects; neutrinos emitted at deep position, which are experienced significant acceleration,

---

[7] The total cross section of neutrino-electron inelastic scattering is Burrows & Thompson (2002)

$$\sigma_{\rm e} \sim \frac{3}{8}\sigma_0\frac{\varepsilon_\nu kT}{(m_{\rm e}c^2)^2},$$

where $\sigma_0 \sim 1.7\times10^{-44}$ cm^2 is reference neutrino cross section, $m_{\rm e}$ is the electron mass, T is the temperature of electrons. On the other hand, the total cross section of neutron-neutrino elastic scattering is

$$\sigma_{\rm n} \sim \frac{\sigma_0}{4}\left(\frac{\varepsilon_\nu}{m_{\rm e}c^2}\right)^2.$$

The reason why we employ the cross section for neutrons is that due to the electron capture ($p + e^- \to n + \nu_{\rm e}$) the neutron fraction increases, whereas the proton fraction decreases inside the neutrinosphere. Therefore, neutrons are dominant target particle for propagating neutrinos. However, it should be noted that the total cross section of proton-neutrino scattering differs from neutron only $\sim 20\%$.

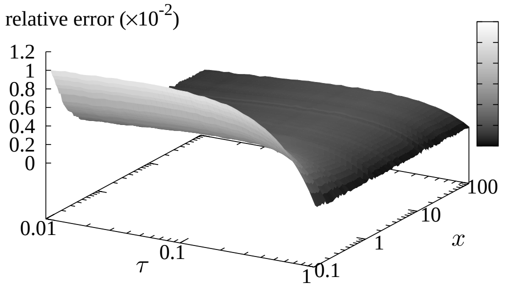

Figure A1. Absolute value of the relative error of the numerical solution in the case of $\tau_0 = 1$.

can more easily escape than the spherically symmetric configuration, while the acceleration might not complete due to the earlier escape. To give more concrete result, more detailed calculation is strongly required.

ACKNOWLEDGMENTS

We thank K. Asano, K. Kiuchi, H. Okawa, Y. Sekiguchi, M. Shibata, and T. Takiwaki for stimulating discussion and M. Suwa for proofreading. This work has been supported in part by the Grants-in-Aid for the Scientific Research from the Ministry of Education, Science and Culture of Japan (No. 23840023) and HPCI Strategic Program of Japanese MEXT.

APPENDIX A: TEST CALCULATION

In this section, we show a test result of our numerical calculation. A special solution of Eq. (7) is given by

$$f_\nu(\tau, x) = \tau^{5/2} x^{-10}, \tag{A1}$$

with $j = 0$ and adequate boundary conditions. In Fig. A1, we show the absolute value of the relative error, |1-(numerical solution)/(exact solution)| in the case where $\tau_0 = 1$ as an example. The grid setup is the same as one used in Sec. 3.4. We find that the relative error is always less than $\sim 10^{-2}$ for (A1). Hence, the error does not affect the conclusion in §4.

REFERENCES

Asano K., Fukuyama T., 2000, ApJ, 531, 949

Asano K., Fukuyama T., 2001, ApJ, 546, 1019

Bethe H. A., 1990, Reviews of Modern Physics, 62, 801

Blandford R. D., Payne D. G., 1981, MNRAS, 194, 1033

Bruenn S. W., Mezzacappa A., Hix W. R., et al., 2009, in American Institute of Physics Conference Series, edited by G. Giobbi, A. Tornambe, G. Raimondo, M. Limongi, L. A. Antonelli, N. Menci, & E. Brocato, vol. 1111 of American Institute of Physics Conference Series, 593–601

Buras R., Rampp M., Janka H.-T., Kifonidis K., 2006, A&A, 447, 1049

Burrows A., Livne E., Dessart L., Ott C. D., Murphy J., 2006, ApJ, 640, 878

Burrows A., Thompson T. A., 2002, arXiv:astro-ph/0211404

Chen W.-X., Beloborodov A. M., 2007, ApJ, 657, 383

Dessart, L., Ott, C. D., Burrows, A., Rosswog, S., & Livne, E. 2009, ApJ, 690, 1681

Di Matteo T., Perna R., Narayan R., 2002, ApJ, 579, 706

Goodman J., Dar A., Nussinov S., 1987, ApJ, 314, L7

Horiuchi S., Beacom J. F., Dwek E., 2009, Phys. Rev. D, 79, 8, 083013

Janka H., 1995, Astroparticle Physics, 3, 377

Janka H., 2001, A&A, 368, 527

Kawanaka N., Mineshige S., 2007, ApJ, 662, 1156

Liebendörfer M., Mezzacappa A., Thielemann F.-K., Messer O. E., Hix W. R., Bruenn S. W., 2001, Phys. Rev. D, 63, 10, 103004

MacFadyen A. I., Woosley S. E., 1999, ApJ, 524, 262

Nagataki S., Takahashi R., Mizuta A., Takiwaki T., 2007, ApJ, 659, 512

Payne D. G., Blandford R. D., 1981, MNRAS, 196, 781

Popham R., Woosley S. E., Fryer C., 1999, ApJ, 518, 356

Press W. H., Teukolsky S. A., Vetterling W. T., Flannery B. P., 1992, Numerical recipes in FORTRAN. The art of scientific computing

Raffelt G. G., 2001, ApJ, 561, 890

Rybicki G. B., Lightman A. P., 1979, Radiative processes in astrophysics

Setiawan S., Ruffert M., Janka H.-T., 2006, A&A, 458, 553

Shibata M., Kiuchi K., Sekiguchi Y., Suwa Y., 2011, Progress of Theoretical Physics, 125, 1255

Sumiyoshi K., Yamada S., 2012, ApJS, 199, 17

Sumiyoshi K., Yamada S., Suzuki H., Shen H., Chiba S., Toki H., 2005, ApJ, 629, 922

Suwa Y., Kotake K., Takiwaki T., Whitehouse S. C., Liebendörfer M., Sato K., 2010, PASJ, 62, L49

Suwa Y., Murase K., 2009, Phys. Rev. D, 80, 123008

Zalamea I., Beloborodov A. M., 2011, MNRAS, 410, 2302